

Paramagnetic Susceptibility in the V_3Si Type of Compounds in the Normal State

J. LABBÉ*

Laboratoire de Physique des Solides associé au Centre National de la Recherche Scientifique,
Faculté des Sciences d'Orsay, Orsay, France

(Received 28 December 1966)

Tight-binding calculations, applied to a linear-chain model, give a rough description of the d -band structure of the V_3Si type of compounds, with very high peaks in the density of states. The Fermi level should fall in one of these peaks. This leads to a large and strongly temperature-dependent Pauli susceptibility. The orbital Van Vleck susceptibility is discussed with respect to the position of the Fermi level in the d band.

INTRODUCTION

IN the V_3Si type of compounds which have a high superconducting transition temperature T_c , the paramagnetic susceptibility and the Knight shift exhibit an unusually strong temperature dependence.¹ Figures 1 and 2 show the experimental results for V_3Si . The susceptibility χ decreases very quickly as the temperature increases. However, at room temperature, its value remains fairly high. For the vanadium nuclei the Knight shift k_V has a positive value and it increases with increasing temperature. More recently, in V_3Si Gossard² discovered the effect, on the nuclear-magnetic-resonance properties, of the low-temperature structural transformation earlier observed by Bateman and Barrett.³ The temperature T_m , at which this transformation begins, is higher by several degrees than the superconducting transition temperature T_c . The structural transformation therefore occurs in the *normal state*. The stable phase is cubic at $T > T_m$ and tetragonal at $T < T_m$. The distortion amplitude ϵ is about 10^{-3} to $2 \cdot 10^{-3}$ times the lattice parameter. The volume of the unit cell remains constant during the transformation. At temperature lying between T_c and T_m , Gossard observed a splitting in the NMR spectrum of the V^{51} nuclei.

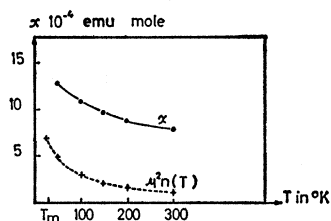


FIG. 1. Temperature dependence of the measured susceptibility in V_3Si . The full line shows the measured total susceptibility χ . The dashed line shows the calculated d -electron Pauli susceptibility $\mu^2 n(T)$, without exchange.

* This work is a part of a thesis which will be submitted by J. Labbé to the Faculté des Sciences d'Orsay, in partial fulfillment of the requirements for the Doctorat d'Etat ès Sciences Physiques.

¹ A. M. Clogston, A. C. Gossard, V. Jaccarino, and Y. Yafet, *Rev. Mod. Phys.* **36**, 170 (1964); *Phys. Rev. Letters* **9**, 262 (1962).

² A. C. Gossard, *Phys. Rev.* **149**, 246 (1966).

³ B. W. Batterman and C. S. Barrett, *Phys. Rev.* **145**, 296 (1966).

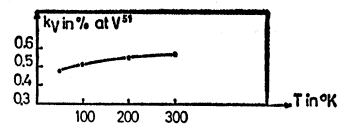
Here we want to show that these experimental results can be understood with a simple model.⁴ In this paper we shall compute the Pauli and Van Vleck susceptibilities in the cubic phase. In a second paper we shall apply our results to calculate the Knight shift in the two phases.

1. SIMPLE MODEL FOR BAND STRUCTURE IN CUBIC PHASE

In the cubic phase, the crystal has the β -tungsten, or A-15, structure (Fig. 3). The vanadium atoms form an array of dense linear chains running in the $[100]$, $[010]$, and $[001]$ directions. The silicon atoms form a body-centered cubic lattice. In the Hartree approximation, we use a narrow d -band system analyzed in tight binding and a broad conduction s band. In this approach, the crystal can be considered, for the d electrons, as an assembly of one-dimensional crystals. The cohesion of the whole lattice is due to the tridimensional s electrons of the transitional and nontransitional atoms. The density of state $n(E)$, resulting from this structure, is shown in Fig. 4. There are three d sub-bands. In this crude model, the value of $n(E)$ is infinite at the two edges of a d sub-band. The d -band density of states is the superposition of the contributions from all the linear chains, so that there is a very large degeneracy for the d band.

Specific-heat measurements⁵⁻⁷ show that the V_3X compounds, with high superconducting transition temperature T_c , have unusually large values of the electronic specific heat, leading to very large densities of states $n(E_F)$ at the Fermi level. The Fermi level should therefore be placed on one of the peaks of the Fig. 4. For instance, in V_3Si , the valency of V atoms makes it

FIG. 2. Temperature dependence of the measured Knight shift in V_3Si .



⁴ J. Labbé and J. Friedel, *J. Phys. Radium* **27**, 153 (1966).

⁵ F. J. Morin and J. P. Maita, *Phys. Rev.* **129**, 115 (1963).

⁶ J. E. Kunzler, J. P. Maita, H. J. Levinstein, and E. J. Ryder, *Phys. Rev.* **143**, 390 (1966).

⁷ J. Bonnerot (to be published).

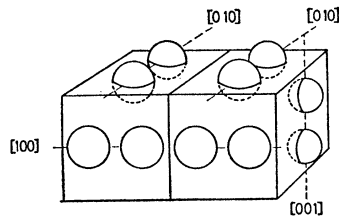


FIG. 3. The A-15 crystal structure: The spheres represent vanadium atoms; the Si atoms would be at the corners and at the center of the cube.

reasonable to assume the Fermi level to be on the third peak from the left, i.e., the narrowest sub-band to be nearly empty.

2. FINE BAND STRUCTURE ASSOCIATED WITH DISTORTION

Using this d -band model, we discussed in Ref. 4 the stability of the cubic structure with respect to a uniform distortion. It was shown that a tetragonal distortion could make the energy decrease, when the Fermi level was sufficiently close to a peak. In such a distortion, the degeneracy is partly lifted, each peak splitting into two peaks (Fig. 5). In V_3Si , the stable phase, at absolute zero, is tetragonal with a lengthening of the unit cell in the $[100]$ direction. The chains running in this direction are stretched. On these chains, the d bands become narrower. In the two other directions the chains contract and the d bands become wider. The peak, on which the Fermi level lies in the cubic phase, splits into a $[100]$ peak and a doubly degenerate $[010]$ and $[001]$ peak (Fig. 6). It can be shown that, in the stable state,

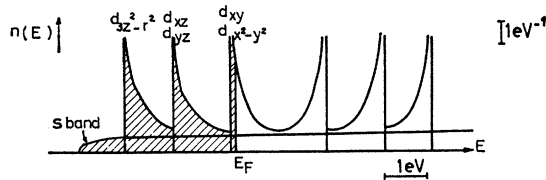


FIG. 4. Density of states in the cubic phase, calculated in tight binding.

the Fermi level E_F lies between the bottoms E_{m1} and E_{m2} of these two peaks. We shall see that a rough estimate, using the numerically known values of the parameters in V_3Si , leads to $E_{m1} - E_F \approx 3.10^{-3} \text{ eV}$. This rather fine structure is very sensitive to the temperature. By an increase in the temperature, from absolute zero to about 20°K , the occupancy of the states of the $[100]$ sub-band (Fig. 6) becomes appreciable. This leads to a decrease in the stability of the tetragonal phase. Calculations give the right order of magnitude for the temperature T_m of the structural transformation.⁸ The general features of the variation of the distortion ϵ with the temperature, below T_m , are found in fairly good agreement with experiments. In our model, the transformation is found to be first order, but with only small discontinu-

ties of the physical parameters, such as distortion, shear modulus, and so on. These discontinuities may be so small that even a very small dispersion in the values of T_m , due to crystal inhomogeneities, is sufficient to mask them. In fact, experimentally, the transformation does not exhibit the specific-heat peak characteristic of a second-order phase transition.

3. CHOICE OF NUMERICAL VALUES OF PARAMETERS IN V_3Si

The actual value of the density of states $n(E_F)$ at Fermi level in V_3Si is difficult to estimate because of the electron-phonon enhancement already discussed by Clogston.⁹ On the other hand, we made a mistake in our Ref. 8.

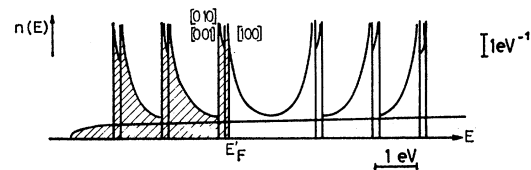


FIG. 5. Density of states in the tetragonal phase.

We had attributed to the tetragonal phase the value resulting from the low-temperature specific-heat measurements of Morin and Maita.⁵ More recent measurements^{6,7} show that this value holds for the cubic phase. As an upper limit, we shall use the value $n(E_F) \approx 10 \text{ eV}^{-1}$ per vanadium atom and for the two spin directions, in the cubic phase.

Now, the Slater coefficient q , which determines the radial dependence of the d atomic wave functions, is given by Eq. (II, 14) in Ref. 8. We find $q \approx 0.27 \text{ \AA}^{-1}$. On the other hand, Eq. (II, 13) in Ref. 8 imposes severe limitations on the choice of the sub-band width $2|E_m|$. We find $7.2 \text{ eV} < 2|E_m| < 9.6 \text{ eV}$. But, if we want to be in the case b of our discussion in Ref. 4 (i.e., where the cubic phase is unstable at 0°K , and not metastable), $|E_m|$ must satisfy $7.9 \text{ eV} < 2|E_m| < 9.6 \text{ eV}$. In our calculations we have chosen the width $2|E_m| = 9 \text{ eV}$. The number Q of electrons in the nearly empty d sub-band is thus $Q \approx 16/\pi^2 |E_m| n(E_F) \approx 0.036$ electrons per vanadium atom, against 4 available states per vanadium atom.

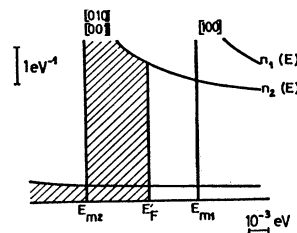


FIG. 6. Fermi-level position in the tetragonal phase of V_3Si .

⁸ J. Labbé and J. Friedel, J. Phys. Radium 27, 303 (1966).

⁹ A. M. Clogston, Phys. Rev. 136, 8 (1964).

Using the above numerical values of the parameters, computer calculations described in Ref. 8 give us a structural transformation temperature $T_m \simeq 23.2^\circ\text{K}$. The calculated variation of the distortion amplitude ϵ with the temperature is shown in Fig. 7. The discontinuity in ϵ at T_m is only 8×10^{-5} , i.e., about 20 times smaller than the value at 0°K . These results are in better agreement with experimental data³ than those found with our first choice of the parameters values in Ref. 8.

Here, we may notice that we find, for the Slater coefficient q , a numerical value much smaller than in the free vanadium atom (where it is about 1 \AA^{-1}) and also probably smaller than in pure vanadium metal. This means that the d atomic wave functions are more extended in space in V_3Si than in vanadium metal. This can be understood from the fact that, in a linear chain in V_3Si , the distance between two neighboring vanadium atoms is smaller than in pure metal (2.36 \AA against 2.63 \AA). Indeed, the rather large value, which we find for the d sub-band width $2|E_m|$, is consistent with the increase in overlapping which must result from atomic wave functions more extended in space. But we must keep in mind that the tight-binding approach is all the more rough as overlapping is stronger.

4. PARAMAGNETIC SUSCEPTIBILITY IN CUBIC PHASE

With our assumption that the Fermi level lies on a d -band peak in the density of states, we can neglect the s -electrons contribution to $n(E_F)$. Thus the paramagnetic susceptibility is made of two main contributions. On the one hand, a large Pauli susceptibility $\chi_d(T)$, strongly decreasing with increasing temperature, is expected from the d states lying close to the Fermi level. On the other hand, the d -band structure, made of neighboring and partly occupied sub-bands, leads to a large orbital susceptibility χ_0 , nearly independent of the temperature. If we neglect the diamagnetic contribution, the whole susceptibility can be written

$$\chi = \chi_0 + \chi_d(T). \quad (1)$$

A. Pauli Susceptibility, Calculated in our Model, for V_3Si

In this calculation we shall neglect all the contributions to the density of states, except the one provided by the nearly empty d sub-band (Fig. 4). The neglected contributions (s band and others d sub-band) only give rise to small and weakly temperature-dependent terms in the Pauli susceptibility. In our approximation, as we have shown in Ref. 4, we must use the expression of the density of states

$$n(E) = (Z/\pi)(E_m^2 - E^2)^{-1/2}, \quad (2)$$

where Z is a normalization constant (for a d_{xy}, x^2-y^2 sub-band we have $Z=4$ electronic states per vanadium atom). In V_3Si , the Fermi level is very near the bottom

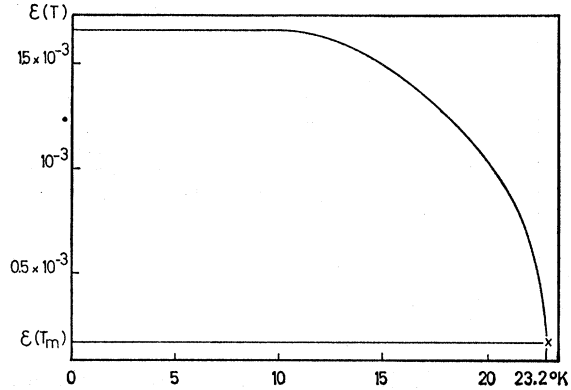


FIG. 7. Calculated distortion amplitude ϵ , as a function of the temperature.

E_m of the sub-band. As usual in transition elements, we must take into account the exchange enhancement. Thus the Pauli susceptibility is given by the formula¹⁰

$$\chi_d(T) = \mu^2 n(T) / (1 - Jn(T)). \quad (3)$$

Here J arises from exchange interactions, μ is the Bohr magneton, and, as shown in Appendix A, $n(T)$ is given by

$$n(T) = - \int_{E_m}^{-E_m} f'(E) n(E) dE, \quad (3')$$

where $f'(E)$ is the derivative with respect to E of the Fermi function $f(E) = (1 + e^{(E-E_F)/kT})^{-1}$. Of course, the Fermi level E_F is a function of the temperature. We shall neglect the electronic transfer towards the s band and the other d sub-bands. At a given temperature T , we must therefore calculate E_F by writing the number of electrons in the sub-band to be a constant. This gives

$$\int_{E_m}^{-E_m} n(E) f(E) dE = Q. \quad (4)$$

Using the numerical values of Sec. 3, we have, at absolute zero, for V_3Si , $E_F(0) - E_m \simeq 18.10 \times 10^{-4} \text{ eV}$. A critical value of T is T_0 such that $kT_0 = E_F(0) - E_m$. Here, we have $T_0 \simeq 21^\circ\text{K}$. In Appendix B we give the usual expansion of $\mu^2 n(T)$, for small temperatures, in $(T/T_0)^2$. But it would be valid only for $T \ll T_0$, i.e., very close to absolute zero, in the superconducting state, where the pairing makes $\chi_d(T)$ vanish. In Appendix C we give an expansion of $\mu^2 n(T)$, for large temperatures, in T_0/T , and we show that it is valid for $T > 100^\circ\text{K}$. Here we are interested in all the values of T in the normal state, including T of the same order as T_0 . E_F and $\chi_d(T)$ must therefore be computed numerically using Eqs. (4), (3) and (3'). Figure 1 shows the calculated temperature variations of $\mu^2 n(T)$. If we assume that J keeps a reasonable value, we see that, between 50 and 400°K , our

¹⁰ A. M. Clogston, V. Jaccarino, and Y. Yafet, Phys. Rev. **134**, A650 (1964).

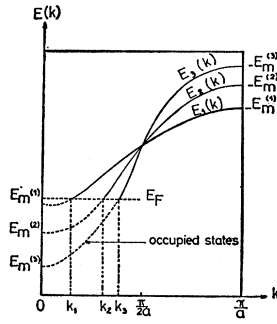


FIG. 8. The d -band structure of a linear chain in E versus k diagram.

results are in fairly good agreement with experiment. It would be interesting to do very careful measurements between T_m and 50°K. At room temperature, $\mu^2 n(T)$ is about seven times smaller than at T_m , and its residual value is only (at 300°K) $1 \cdot 10^{-4}$ emu mole $^{-1}$. Experimentally, the whole susceptibility at room temperature is about $8 \cdot 10^{-4}$ emu mole $^{-1}$. Thus, on the assumption of Eq. (1), an upper limit for the orbital contribution χ_0 is about $6 \cdot 10^{-4}$ emu mole $^{-1}$. In fact, because of the nearly temperature-independent contributions from the s band and the other d sub-bands to the Pauli susceptibility, χ_0 is probably smaller than this value.

It is very easy to show that all the results of this section would be the same for a nearly full d sub-band. Indeed, we see from (2) that $n(E)$ is a symmetrical function of E . When Q becomes $Z-Q$ in (4), E_F becomes $-E_F$, and χ remains unchanged by (3), as can be seen from the well-known properties of the Fermi function.

B. Calculation of Orbital Paramagnetic Susceptibility in our Model

Kubo has shown how to apply Van Vleck's second-order perturbation to the orbital paramagnetic susceptibility in metals.¹¹ The susceptibility χ_0 found in this way is of the order of μ^2/Δ , where μ is the Bohr magneton and Δ is the mean separation of the energy levels connected by the orbital angular momentum. Thus, it is clear that only narrow bands (in our case, the d band) will give rise to an appreciable orbital contribution. On the other hand, because Δ is of the order of 1 eV, χ_0 will be nearly temperature-independent.

In the most general case of a metal with a tridimensional narrow band structure, this theory leads to rather tedious calculations. But, in our model, we may simply add the d -band contributions from all the linear chains of vanadium atoms. For a linear chain, the orbital susceptibility is a very anisotropic tensor. But for the whole crystal, in the cubic phase, χ_0 is isotropic. In the following, we shall neglect the spin-orbit coupling.

Let us consider a linear chain of a large number N of vanadium atoms, with an interatomic distance a . In tight binding, the d band is made of 3 degenerate sub-

bands (Fig. 4). The Bloch function for a state g , of wave vector k , of the n th sub-band ($n=1, 2, 3$), can be written

$$|n, g, k\rangle = \frac{1}{\sqrt{N}} \sum_v \psi_{n,g}(\mathbf{r}-v\mathbf{a}) e^{ikv\mathbf{a}}, \quad (5)$$

where $\psi_{n,g}(\mathbf{r}-v\mathbf{a})$ is a d atomic wave function, centered on the v th atom in the chain and normalized to unity. The energy $E_n(k)$ of a state of the n th sub-band is a sinusoidal function of the wave number k . It is given by

$$E_n(k) = E_m^{(n)} \cos ka, \quad (E_m^{(n)} < 0). \quad (6)$$

In Fig. 8 we have plotted the energy as a function of k for the 3 sub-bands.

Now, calling Oz the axis of the chain, we apply a magnetic field \mathbf{H} . The contribution to the magnetic free energy due to the orbital susceptibility is

$$F = \mu^2 \sum_{n < n'} \sum_{g, g'} \sum_k \frac{|\langle ngk | \mathbf{H} \cdot \mathbf{L} | n'g'k \rangle|^2}{E_n(k) - E_{n'}(k)} \times \{f[E_n(k)] - f[E_{n'}(k)]\}, \quad (7)$$

where $f(E)$ is the Fermi function. The orbital susceptibility of the chain is therefore a 2-rank symmetrical tensor $\chi_{\alpha\beta}$ defined by

$$F = -\frac{1}{2} \sum_{\alpha\beta} \chi_{\alpha\beta} H_\alpha H_\beta, \quad (\alpha, \beta = x, y, z), \quad (8)$$

with

$$\chi_{\alpha\beta} = 2\mu^2 \sum_{n < n'} \sum_{g, g'} \sum_k \frac{\langle ngk | L_\alpha | n'g'k \rangle \langle n'g'k | L_\beta | ngk \rangle}{E_n(k) - E_{n'}(k)} \times \{f[E_{n'}(k)] - f[E_n(k)]\}, \quad (9)$$

and, from (5),

$$\langle ngk | L_\alpha | n'g'k \rangle = \frac{1}{N} \sum_{vv'} \langle \psi_{n,g}(\mathbf{r}-v\mathbf{a}) | L_\alpha | \psi_{n',g'}(\mathbf{r}-v'\mathbf{a}) \rangle e^{ik(v'-v)\mathbf{a}}. \quad (10)$$

In tight binding, we can neglect all the terms with $v \neq v'$. The k dependence then disappears from (10). Moreover, because of the periodicity, the remaining terms in (10) do not depend on v , and we get

$$\langle ngk | L_\alpha | n'g'k \rangle = \langle \psi_{n,g} | L_\alpha | \psi_{n',g'} \rangle,$$

where $\psi_{n,g}$ is the d atomic wave function of the state g of the n th sub-band, centered at the site $v=0$. Finally,

$$\chi_{\alpha\beta} = 2\mu^2 \sum_{n < n'} \sum_{g, g'} \langle \psi_{n,g} | L_\alpha | \psi_{n',g'} \rangle \langle \psi_{n',g'} | L_\beta | \psi_{n,g} \rangle \frac{Na}{\pi} \int_0^{\pi/a} \frac{f[E_{n'}(k)] - f[E_n(k)]}{E_n(k) - E_{n'}(k)} dk. \quad (11)$$

According to the conventions of Fig. 8, the values 1, 2, and 3 of n respectively correspond to the sub-bands

¹¹ R. Kubo and Y. Obata, J. Phys. Soc. Japan 11, 547 (1956).

$d_{x^2-y^2}d_{xy}$, $d_{xz}d_{yz}$, and $d_{3z^2-r^2}$. The degeneracies of these sub-bands are of spin and orbital origin. Thus the index g can take four values for $n=1$ or 2, and two values for $n=3$. The matrix elements in (11) are easy to calculate. The operators L_α only connect states with the same spin orientation. The component L_z is diagonal and does not contribute. The components L_x and L_y only connect states for which the magnetic quantum numbers differ by ± 1 . We use the fact that the ψ_{ng} in (11) are normalized to unity. Detailed calculations are given in Appendix D. The final result, for the orbital susceptibility of a linear chain in the 0z or [001] direction, is¹²

$$(\chi_{\alpha\beta})_{001} = \begin{pmatrix} \Lambda & 0 & 0 \\ 0 & \Lambda & 0 \\ 0 & 0 & 0 \end{pmatrix}, \quad (12)$$

with

$$\Lambda = \chi_{xx} = \chi_{yy} = 2\mu^2 \frac{Na}{\pi} \left\{ 4 \int_0^{\pi/a} \frac{f[E_2(k)] - f[E_1(k)]}{E_1(k) - E_2(k)} dk + 6 \int_0^{\pi/a} \frac{f[E_3(k)] - f[E_2(k)]}{E_2(k) - E_3(k)} dk \right\}. \quad (13)$$

For the chains running in the two other directions, we have, by analogy with (12),

$$(\chi_{\alpha\beta})_{010} = \begin{pmatrix} \Lambda & 0 & 0 \\ 0 & 0 & 0 \\ 0 & 0 & \Lambda \end{pmatrix} \quad \text{and} \quad (\chi_{\alpha\beta})_{100} = \begin{pmatrix} 0 & 0 & 0 \\ 0 & \Lambda & 0 \\ 0 & 0 & \Lambda \end{pmatrix}.$$

We see from (12) that, when a magnetic field is applied, the orbital magnetic moment induced in a linear chain of vanadium atoms is orthogonal to the chain. But all the chains of the crystal geometrically add their moments and the resultant is parallel to the field. So the orbital susceptibility χ_0 of the crystal is isotropic:

$$\chi_0 = (\chi_{\alpha\beta})_{001} + (\chi_{\alpha\beta})_{010} + (\chi_{\alpha\beta})_{100} = 2\Lambda.$$

At absolute zero, the Fermi function $f(E)$ is equal to 1 for $E < E_F$ and 0 for $E > E_F$. Let k_1, k_2, k_3 be the values of k at the Fermi level E_F , respectively, in the 3 d sub-bands (Fig. 8). We want to give here a result valid when E_F is anywhere in the band. Thus we must consider all the cases, $k_1 < k_2 < k_3$, $k_2 < k_1 < k_3$, \dots . We shall use the notations $\sup(k_1 k_2)$ and $\inf(k_1 k_2)$, respec-

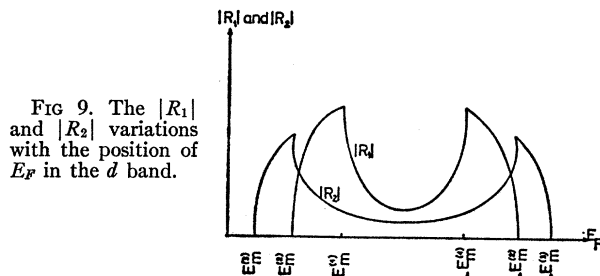
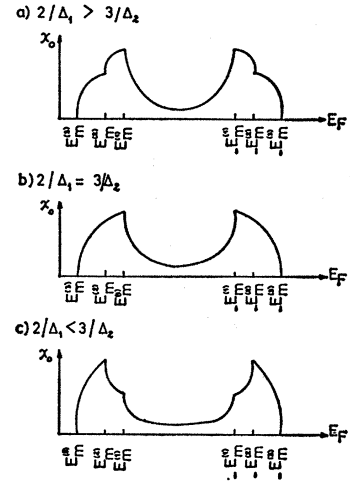


FIG. 9. The $|R_1|$ and $|R_2|$ variations with the position of E_F in the d band.

¹² Henceforward, N will be the total number of vanadium atoms contained in all the chains of the crystal parallel to one direction; thus the total number of vanadium atoms in the whole crystal will be $3N$.

FIG. 10. Variations of the orbital susceptibility χ_0 with the position of E_F in the d band.



tively, for the largest and the smallest of k_1 and k_2 . From (6) and (13) we find

$$\chi_0 = 2\Lambda = 4\mu^2 \frac{Na}{\pi} \left\{ 4 \int_{\inf(k_1 k_2)}^{\sup(k_1 k_2)} \frac{dk}{|(E_m^{(1)} - E_m^{(2)}) \cos ka|} + 6 \int_{\inf(k_2 k_3)}^{\sup(k_2 k_3)} \frac{dk}{|(E_m^{(2)} - E_m^{(3)}) \cos ka|} \right\}. \quad (14)$$

We shall put $E_m^{(1)} - E_m^{(2)} = \Delta_1$, $E_m^{(2)} - E_m^{(3)} = \Delta_2$. By performing the integrations in (14), we get

$$\chi_0 = 3N \frac{4\mu^2}{3\pi} \left\{ \frac{4}{\Delta_1} |R_1| + \frac{6}{\Delta_2} |R_2| \right\}, \quad (15)$$

with

$$R_1 = \ln \left| \frac{(\tan(k_2 a/2) + 1)(\tan(k_1 a/2) - 1)}{(\tan(k_2 a/2) - 1)(\tan(k_1 a/2) + 1)} \right|, \quad (16)$$

$$R_2 = \ln \left| \frac{(\tan(k_3 a/2) + 1)(\tan(k_2 a/2) - 1)}{(\tan(k_3 a/2) - 1)(\tan(k_2 a/2) + 1)} \right|. \quad (17)$$

In these equations, k_1, k_2 , and k_3 are related to the Fermi level E_F by

$$E_F = E_m^{(n)} \cos k_n a, \quad n=1, 2, 3 \quad (18)$$

(But we must take $k_n = 0$ when $E_F < E_m^{(n)}$, and $k_n = \pi/a$ when $E_F > E_m^{(n)}$).

The variations of $|R_1|$ and $|R_2|$ with E_F are plotted in Fig. 9. Figure 10 show the corresponding variations of χ_0 , for different cases depending on the values of parameters. The χ_0 variations are symmetrical with respect to the middle of the d band.¹³

When E_F increases from the bottom $E_m^{(3)}$ of the band, $|R_2|$ very quickly increases from zero, with an infinite slope at the beginning. This fact comes from the

¹³ We have neglected the differences, always small in tight binding, between the energies at the middle of the three d sub-bands.

vanishing slope of $E_3(k)$ at the band edge (Fig. 8), leading to an infinite density of states (Fig. 4). So E_F has just to be slightly above the bottom of the d band, for a non-negligible number of electrons to contribute to χ_0 . When E_F gets to the edge $E_m^{(2)}$ of the second sub-band, two antagonistic phenomena occur. On the one hand, $|R_1|$ starts to contribute with an infinite slope. On the other hand, $|R_2|$ starts to decrease with an infinite slope too, because the filling of the second sub-band makes the $E_3(k) \leftrightarrow E_2(k)$ contributions vanish for $k < k_2$. For $2/\Delta_1 > 3/\Delta_2$, the increasing of $|R_1|$ is the strongest, and $d\chi_0/dE_F = +\infty$ at $E_F = E_m^{(2)}$. It can be shown that in this case, χ_0 increases in the whole interval from $E_m^{(2)}$ to $E_m^{(1)}$. For $2/\Delta_1 < 3/\Delta_2$, the decreasing of $|R_2|$ is the strongest, and $d\chi_0/dE_F = -\infty$ at $E_F = E_m^{(2)}$. In this case χ_0 may or may not have a minimum in the interval from $E_m^{(2)}$ to $E_m^{(1)}$, according to the values of parameters. For $2/\Delta_1 = 3/\Delta_2$, there is no discontinuity of the slope $d\chi_0/dE_F$ at $E_F = E_m^{(2)}$, and χ_0 increases up to $E_F = E_m^{(1)}$. When E_F passes above the edge $E_m^{(1)}$ of the third sub-band, $|R_1|$ and $|R_2|$ both decrease, up to the middle of the band. This decrease of χ_0 when the Fermi level approaches the middle of the band is not immediately obvious. Indeed, in this case, the separation of the energy levels, in the denominators in (14), becomes smaller. But the intervals of integration, $|k_2 - k_1|$ and $|k_3 - k_2|$, become smaller too. Therefore, if the contribution from one electron becomes stronger, the number of contributing electrons is reduced. The calculation of the derivative shows that χ_0 is in fact decreasing.

For the same reason, χ_0 keeps a finite value, and remains continuous, when E_F goes through the intersection $k_1a = k_2a = k_3a = \pi/2$ of the sub-bands (Fig. 8). It can easily be shown that, at such a point

$$|R_1| = \ln(E_m^{(2)}/E_m^{(1)}) \quad \text{and} \quad |R_2| = \ln(E_m^{(3)}/E_m^{(2)}).$$

More generally, it is shown in Appendix E that, when E_F is very close to the intersection of two sub-bands, the corresponding contribution to χ_0 varies only slowly with E_F if the second derivatives d^2E/dk^2 , of the two sub-bands at the intersection, are small. Furthermore, the value of χ_0 when E_F is just at the intersection is a simple function of the slopes dE/dk of the two sub-bands. In our case, the sub-band intersections are at the middle of the band (Fig. 8) and the second derivatives d^2E/dk^2 vanish. Thus, when E_F is in the middle part of the band, χ_0 is nearly constant as E_F varies, and its value is given by

$$\chi_0 \simeq 3N \frac{4\mu^2}{3\pi} \left\{ \frac{4}{\Delta_1} \ln \frac{E_m^{(2)}}{E_m^{(1)}} + \frac{6}{\Delta_2} \ln \frac{E_m^{(3)}}{E_m^{(2)}} \right\}. \quad (19)$$

The influence of the temperature, resulting from (13), very much depends on the position of the Fermi level E_F (Fig. 8).

When E_F is far from the middle part of the band, where the sub-bands intersect, the separation of the energy levels which contribute to χ_0 is very large with

respect to kT . Thus χ_0 is nearly temperature independent. This is the case for the V_3Si type of compounds in which $n(E_F)$ is very large and thus E_F is very close to a sub-band edge.

But when E_F is in the middle part of the band, near the sub-band intersections, the separation of the energy levels contributing to χ_0 is small. Thus an increase in the temperature makes the occupancies of these levels become less unsymmetrical. The result is a decrease in the numerators in (13) and thus in χ_0 .

Finally, we give a rough numerical estimation of χ_0 in V_3Si . In Sec. 3 we saw that the major features of the structural transformation were understood in our model, by assuming $E_m^{(1)} \simeq -4.5$ eV for the narrowest d sub-band. This sub-band must be considered as nearly empty. From the measured value of $n(E_F)$, we get $k_1a \simeq 2.8 \cdot 10^{-2}$ rad. For the widths of the others sub-bands, we are reduced to hypothesis. But we have seen that the interatomic distances, in a linear chain of vanadium atoms, is unusually small in all these compounds and that the d -atomic wave functions are strongly extended in space. Thus, the overlapping of two of these wave functions, centered on two neighboring vanadium atoms in a chain, is perhaps not so sensitive to their orientation with respect to the axis of the chain. So the widths of the three sub-bands may be not very different. For instance, we shall assume that $\Delta_1 \simeq 0.5$ eV and $\Delta_2 \simeq 1$ eV. We are in the case a of Fig. 10. From the relations (18), we find $k_2a \simeq 0.45$ rad and $k_3a \simeq 0.72$ rad. This gives us $R_1 = 0.44$, $R_2 = 0.34$ and finally $\chi_0 \simeq 2.3$ emu mole⁻¹. This result must only be considered as an order of magnitude. It can explain at least roughly the high-temperature susceptibility of Fig. 1.

To conclude this section, we shall say that our very rough model leads to:

- (1) a large orbital paramagnetism, nearly temperature independent, when the Fermi level is far from the middle of the d band and
- (2) a small orbital paramagnetism, strongly decreasing as temperature increases, when the Fermi level is near the middle of the d band.

APPENDIX A

In this Appendix we shall not consider exchange enhancement. The usual formula for the susceptibility would give us

$$n(T) = \int_{E_m}^{-E_m} f(E) n'(E) dE, \quad (A1)$$

where $n'(E)$ is the derivative with respect to E of the density of states $n(E)$. But, in our case, $n(E)$ is given by the expression (2), and the formula (A1) is divergent at the bottom E_m of the sub-band. In fact, (A1) is not valid in our case, because the difference $n(E + \mu H) - n(E - \mu H)$, where H is the magnetic field, cannot be

expanded with respect to μH , near the singularity in $n(E)$, at $E = E_m$. Thus, we shall derive the formula (3') in the following way: When the magnetic field is applied, the magnetic moment is given by

$$m = \mu \int_{E_m - \mu H}^{-E_m - \mu H} f(E) n_1(E) dE - \mu \int_{E_m + \mu H}^{-E_m + \mu H} f(E) n_2(E) dE, \quad (\text{A2})$$

where we have introduced

$$\begin{aligned} n_1(E) &= n(E + \mu H), \quad \text{for spins parallel to } \mathbf{H}; \\ n_2(E) &= n(E - \mu H) \quad \text{for spins antiparallel to } \mathbf{H}. \end{aligned}$$

Taking, as new variable, $E_1 = E + \mu H$ in the first integral, and $E_2 = E - \mu H$ in the second integral, we find

$$m = \mu \int_{E_m}^{-E_m} f(E_1 - \mu H) n(E_1) dE_1 - \mu \int_{E_m}^{-E_m} f(E_2 + \mu H) n(E_2) dE_2.$$

This simply gives

$$m = \mu \int_{E_m}^{-E_m} \{f(E - \mu H) - f(E + \mu H)\} n(E) dE. \quad (\text{A3})$$

The Fermi function $f(E)$ having no singularity for $T \neq 0^\circ\text{K}$, we can expand the difference in (A3), and we get

$$m = -2\mu^2 H \int_{E_m}^{-E_m} f'(E) n(E) dE. \quad (\text{A4})$$

If we count $n(E)$ for the two spin directions, the factor 2 disappears from (A4), and we get the formula (3'). Of course, in a case where $n(E)$ would have no singularity, the formula (3') could be deduced from (A1) by integrating by parts.

APPENDIX B

For $T \ll T_0$, the formula (3'), expanded by a well-known method,¹⁴ give us

$$n(T) \simeq n[E_F(0)] \times \left\{ 1 + \frac{\pi^2}{6} \left[\frac{n''}{n} - \left(\frac{n'}{n} \right)^2 \right]_{E_F=E_F(0)} (kT)^2 \dots \right\}. \quad (\text{B1})$$

Making use of expression (2) for $n(E)$, and taking into account that $E_F(0) - E_m$ is small with respect to $|E_m|$, we find

$$n(T) \simeq n[E_F(0)] \left\{ 1 + \frac{1}{12} \pi^2 (T/T_0)^2 \dots \right\}. \quad (\text{B2})$$

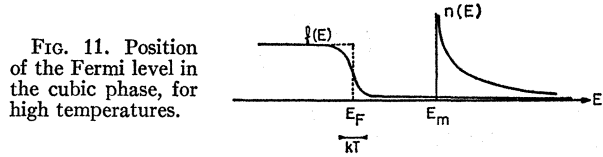
Contrary to the free-electron case, the corrective term

¹⁴ N. F. Mott and H. Jones, *The Theory of the Properties of Metals and Alloys* (Oxford University Press, London, 1900), p. 186.

in (B2) is positive. In fact, in V_3Si , $T_0 \simeq 21^\circ\text{K}$ and (B2) would be valid only for very small temperatures, in the superconducting state. It therefore has no physical meaning.

APPENDIX C

In the case where $T \gg T_0$, let us search the temperature values for which the electrons in the sub-band begin to behave as a Boltzmann gas. Such a behavior is obtained when the Fermi level E_F goes away, far below the bottom E_m of the sub-band, as shown on Fig. 11,



the difference $E_m - E_F$ becoming much larger than kT . In this case $(E_F - E_m)/kT$ is negative with an absolute value much larger than unity, and we have $\exp(E_F - E_m)/kT \ll 1$. So the Fermi function can be expanded as

$$f(E) = \exp\left(\frac{E_F - E}{kT}\right) - \exp\left(\frac{E_F - E}{2kT}\right) + \exp\left(\frac{E_F - E}{3kT}\right) \dots (-)^{p-1} \exp\left(\frac{E_F - E}{pkT}\right) \dots \quad (\text{C1})$$

Thus Eq. (4), which determines the Fermi level, can be written

$$\sum_{p=1}^{\infty} (-)^{p-1} \exp\left(\frac{E_F - E_m}{pkT}\right) \int_{E_m}^{-E_m} n(E) \times \exp\left(-p \frac{E - E_m}{kT}\right) dE = Q. \quad (\text{C2})$$

In fact, the $n(E)$ values very far above the bottom E_m of the sub-band are of little account, and we may replace the expression (2) by

$$n(E) \simeq (Z/\pi) (2|E_m|)^{-1/2} (E - E_m)^{-1/2}, \quad (\text{C3})$$

where the upper limit of the integrals in (C2) are replaced by infinity. So the gamma function $\Gamma(\frac{1}{2})$ appears in (C2), which becomes

$$\begin{aligned} & \exp\left(\frac{E_F - E_m}{kT}\right) - 2^{-1/2} \exp\left(\frac{E_F - E_m}{2kT}\right) \\ & + 3^{-1/2} \exp\left(\frac{E_F - E_m}{3kT}\right) \dots (-)^{p-1} p^{-1/2} \\ & \times \exp\left(\frac{E_F - E_m}{pkT}\right) \dots = \frac{2}{\sqrt{\pi}} \left(\frac{T_0}{T}\right)^{1/2}. \quad (\text{C4}) \end{aligned}$$

The Eq. (C4) determines the Fermi level. For $T \gg T_0$, it can be solved by approximations. We get

$$\exp \frac{E_F - E_m}{kT} \simeq \frac{2}{\sqrt{\pi}} \left(\frac{T_0}{T} \right)^{1/2} \left\{ 1 + \left(\frac{2}{\pi} \right)^{1/2} \left(\frac{T_0}{T} \right)^{1/2} \dots \right\}. \quad (C5)$$

The Pauli susceptibility can be expanded in the same way. We find

$$\begin{aligned} n(T) \simeq & \frac{Z}{(2\pi kT |E_m|)^{1/2}} \exp \left(\frac{E_F - E_m}{kT} \right) \\ & \times \left\{ 1 - 2^{1/2} \exp \left(\frac{E_F - E_m}{kT} \right) \right. \\ & + 3^{1/2} \exp \left(2 \frac{E_F - E_m}{kT} \right) \dots (-)^{p-1} p^{1/2} \\ & \left. \times \exp \left(p \frac{E_F - E_m}{kT} \right) \dots \right\}. \quad (C6) \end{aligned}$$

Inserting (C5) into (C6), we obtain

$$n(T) \simeq \frac{Q}{kT} \left\{ 1 - \left(\frac{2}{\pi} \right)^{1/2} \left(\frac{T_0}{T} \right)^{1/2} \dots \right\}. \quad (C7)$$

APPENDIX D

We shall use the notation $+$ and $-$ for the two spin states. The nonvanishing inter-sub-band matrix elements only are

$$\begin{aligned} \langle d_{xz'} + |L_x| d_{x^2-y^2'} + \rangle &= 1, & \langle d_{xz'} + |L_y| d_{xy'} + \rangle &= -1, \\ \langle d_{xz'} - |L_x| d_{x^2-y^2'} - \rangle &= 1, & \langle d_{xz'} - |L_y| d_{xy'} - \rangle &= -1, \\ \langle d_{yz'} + |L_x| d_{xy'} + \rangle &= 1, & \langle d_{yz'} + |L_y| d_{x^2-y^2'} + \rangle &= -1, \\ \langle d_{yz'} - |L_x| d_{xy'} - \rangle &= 1, & \langle d_{yz'} - |L_y| d_{x^2-y^2'} - \rangle &= -1, \\ \langle d_{xz'} + |L_x| d_{3z^2-r^2'} + \rangle &= \sqrt{3}, & \langle d_{yz'} + |L_y| d_{3z^2-r^2'} + \rangle &= \sqrt{3}, \\ \langle d_{xz'} - |L_x| d_{3z^2-r^2'} - \rangle &= \sqrt{3}, & \langle d_{yz'} - |L_y| d_{3z^2-r^2'} - \rangle &= \sqrt{3}. \end{aligned}$$

APPENDIX E

Let E_i be the energy at the intersection $k_1 a = k_2 a = r_1$ of two sub-bands $E_1(k)$ and $E_2(k)$. When E_F is close to E_i (Fig. 12), we can use the expansions

$$E_1(k) = E_i + A_1(ka - r_1) + B_1(ka - r_1)^2 + \dots,$$

$$E_2(k) = E_i + A_2(ka - r_1) + B_2(ka - r_1)^2 + \dots$$

We shall suppose that $A_1 \neq A_2$ and $A_1 A_2 > 0$. From (14), the corresponding contribution to χ_0 is propor-

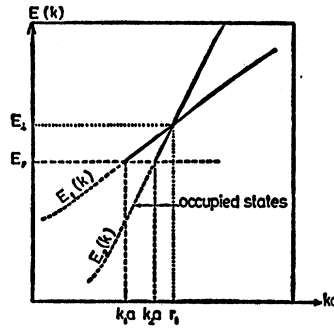


FIG. 12. Case when E_F is close to the intersection of two sub-bands.

tional to the integral

$$I = \int_{\inf(k_1 k_2)}^{\sup(k_1 k_2)} \frac{d(ka)}{|E_1(k) - E_2(k)|},$$

with k_1 and k_2 given by $E_1(k_1) = E_2(k_2) = E_F$. In the two situations, $E_F < E_i$ and $E_F > E_i$, we find

$$\begin{aligned} I = & \frac{1}{A_1 - A_2} \ln \frac{A_1}{A_2} - \frac{1}{A_1 A_2} \left(\frac{B_1}{A_1} + \frac{B_2}{A_2} \right) \\ & \times (E_F - E_i) + O(E_F - E_i)^2. \end{aligned}$$

We see that I , as a function of E_F , is continuous at $E_F = E_i$, as well as its derivatives.

In our case $r_1 = \pi/2$, we have $A_1 = -E_m^{(1)}$, $A_2 = -E_m^{(2)}$, $B_1 = 0$, $B_2 = 0$. Thus, the variation of I near the intersection vanishes at the first order in $E_F - E_i$.